Hybrid Electric Vehicle Propulsion System Architectures of the e-CVT Type

John M. Miller, *Fellow, IEEE*

***Abstract*—There is now significant interest in hybrid electric vehicle (HEV) propulsion systems globally. Economics play a major role as evidenced by oil prices in North America pressing upwards of $100/Bbl coupled with a customer preference for full size crossover and sport utility vehicles. The situation in Oceania is milder, but emerging markets such as China are experiencing automotive sector growth rates of 37%/year. Europe remains least affected by hybrids since nearly 47% of all new vehicles sold are diesel fueled and have economy ratings on par with that of gasoline-electric hybrids. In the global economy there are presently some 57 Mil new vehicles manufactured each year. Toyota and Honda have projected that HEVs will be 10% to 15% of the U.S. market by 2009, with Toyota raising the bar further by stating they will produce 1 Mil hybrids a year in the 2012 time frame. Hybrid propulsion system types are only vaguely comprehended by the buying public, and to a large measure, even by technical professionals. This paper addresses this latter issue by presenting a summary of the globally accepted standard in hybrid power trains—the power split architecture, or more generically and in common usage, the electronic-continuously variable transmission.**

***Index Terms*—Electronic-continuously variable transmission (e-CVT), hybrid electric vehicle (HEV).**

I. Introduction

MOST engineers today, especially those who appreciate vehicles with performance that also are economical to drive, understand the distinction between micro, mild, and full hybrid. This paper will address the situation with full hybrid systems so the first two will be dealt away quickly with some brief remarks. Propulsion system hybridization comes in degrees according to electric power fraction of the overall power plant in the vehicle. Micro, as the name implies, refers to those systems at the low power end of the spectrum. Micro hybrids are the lower book end on propulsion power and contribute on the order of 5% to 10% of fuel economy benefit. Benefit is a relative term as explained in section 1.3.3 of [1] and depends on the value of the base vehicle fuel economy (North American convention) or consumption (Europe and Oceania convention).

An idle-stop system such as may be found on European small cars with an alternator that doubles as a motor for warm restart of the engine via the belt qualifies as a micro hybrid. Power levels of micro hybrids are typically 3 to 5 kW. Mild hybrids are a notch up in power rating, typically 7 to 12 kW and generally have the electric motor-generator located in the vehicle transmission at the engine crankshaft. The Honda Civic and Accord hybrids as well as the GM Silverado pick-up truck are mild hybrids and exhibit economy gains on the order of 10%. By way of architecture, both micro and mild hybrids are classified as parallel type because an uninterrupted mechanical power path connects the engine to the driven wheels. Series hybrids have only an electric power path between the engine and driven wheels. And, series-parallel switching, also known as combination architectures, may use a single electric motor-generator in the vehicle driveline, but with dual clutches that connect the M/G to the engine only, the wheels only, or both. Full hybrids realize 40% and higher fuel economy gains. This paper treats the full (strong) hybrid systems of the power split architecture of both input split and compound split type. Fig. 1 is a top level architectural schematic of the now popular input split e-CVT as developed and introduced into the market by the Toyota Motor Co. In the Toyota Hybrid System (THS) a pair of electric M/Gs provide the electric power circulation path that enables this input split system to deliver mechanical power to the vehicle wheels. High level supervisory control is needed to manage the engine and ac drives under torque control with further coordination provided to the electronically controlled brakes and energy storage system.

Continuously variable transmissions (CVTs) are implemented mechanically, hydraulically and hydromechanically, and electromechanically as depicted in Fig. 2. The various CVT systems have been described in some detail [2]–[4] with the electronic-continuously variable transmission (e-CVT) being an outgrowth of the hydromechanical configuration wherein hydraulics are replaced with ac drives.

A. Power Split e-CVTs of the FirstType: Input Split

The electric, or electronic, CVT is that class of power transmission without need of clutches or step ratio gear shifting. In the e-CVT power flow from the vehicle power plant to the driven wheels is seamless (e.g., no torque interruption) and smooth (no abrupt gear change). Speed differentials that in mechanical transmissions were matched to the generally steady engine speed via ratio changes are now, in the e-CVT, absorbed in the electric variator. A variator is the device in the third tier down in Fig. 2 that is designed to translate the wide speed and torque variations presented to the vehicle driveline via the driven wheels into the restricted speed-torque operating map of the vehicle power plant. Internal combustion engines, regardless of fuel type (gasoline, diesel, hydrogen), operate most efficiently at mid-range speeds and high torque levels. It is one goal of the e-CVT to match the vehicle road load to this engine optimal operating regime.

Fig. 3 shows the high level architecture of the power split e-CVT that is input coupled. Coupling refers to the transmission mechanical ports at which a power splitting device is located. For input split systems such as those now manufactured

Manuscript received April 4, 2005; revised October 26, 2005. Recommended by Associate Editor J. Shen.

The author is with J-N-J Miller Design Services, PLC, Cedar, MI 49621 USA (e-mail: jmmiller35@aol.com).

Digital Object Identifier 10.1109/TPEL.2006.872372

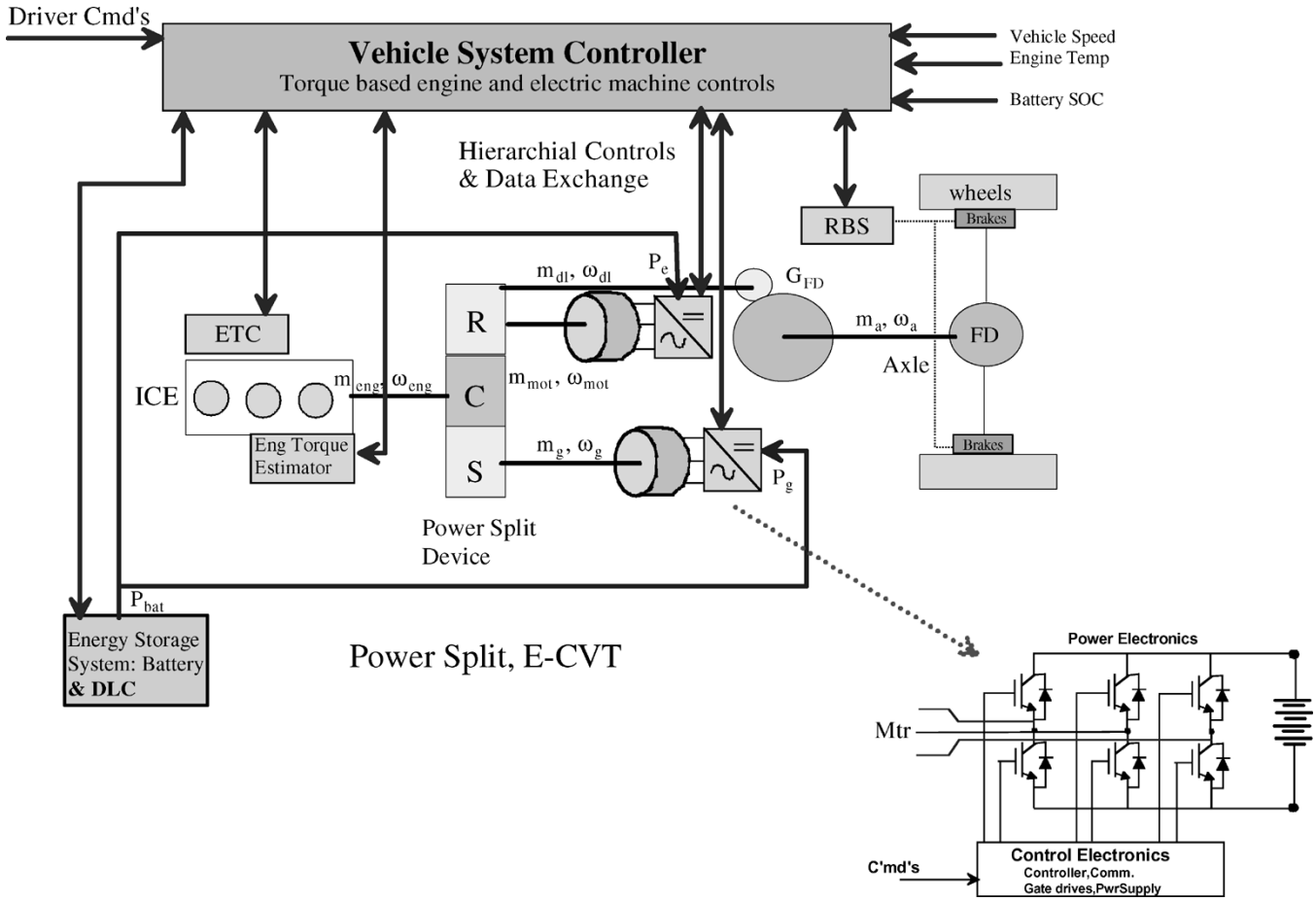

Fig. 1. Power split e-CVT of the input split type.

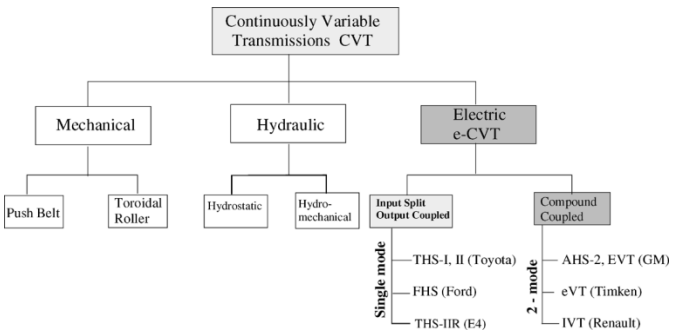

Fig. 2. Classifications of the CVT.

by Toyota and Ford have the power split device at the transmission input, hence, input split.

In the input split, or single mode, system the vehicle engine delivers mechanical power to the wheels via two paths: one a pure mechanical path through the power split device and any output gearing present, then to the wheels, and two, a pure electric path comprising the variator. In an e-CVT the variator consists of a pair of electric motor-generators (M/Gs) that link one of the power split mechanical ports to the output gearing (or a second power split device) mechanical port via a dc link. Electric energy storage may be present on the dc link as either an electrochemical battery or electrochemical capacitor (EC) also known as the ultracapacitor, or double layer capacitor (DLC).

B. Power Split e-CVTs of the Second Type: Compound Split

The second major class of e-CVT shown in Fig. 2 is the compound split configuration distinguished by a pair of mechanical power splitting devices at both the input and output of the transmission (i.e., the mechanical ports). Compound split systems are true four-ports whereas the input split e-CVT is a three-port device because its output mechanical port and its output variator port are one and the same.

Fig. 4 shows the compound split, or as it is sometimes called, the two-mode transmission. Compound split transmissions are e-CVTs under variable structure control. Their description is somewhat more involved, but compound split transmissions in mode 1 are the same as input split with output gearing e-CVTs. That is, the input power split device is a differential and the output power split device is a torque multiplier. Under mode 2 control the compound split e-CVT functions as a full four-port with input and output power split devices both operating as differentials.

To close out this introduction of e-CVT the power split device will be briefly described. The remainder of this paper will then more fully develop the dynamics of input and compound split e-CVTs to reveal the unique requirements each places on the electric path ac drive components.

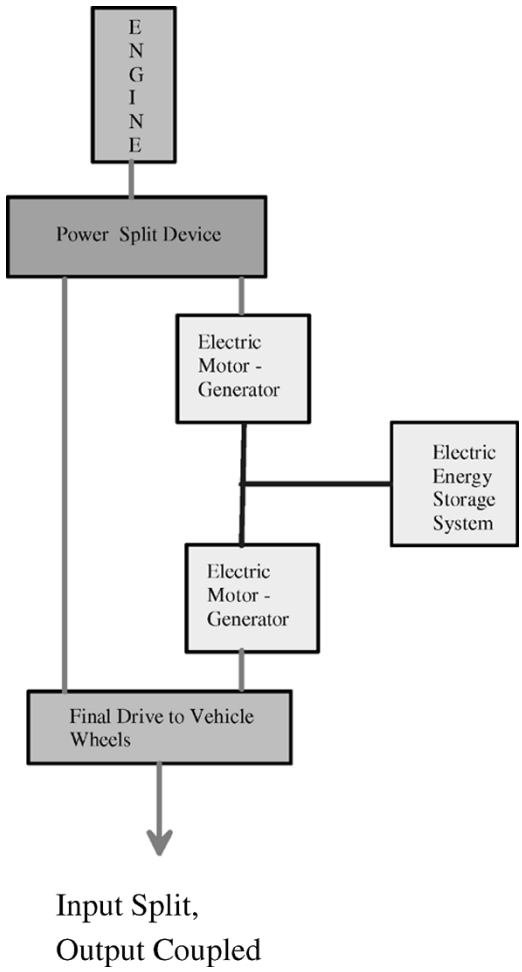

Fig. 3. Input split e-CVT architecture.

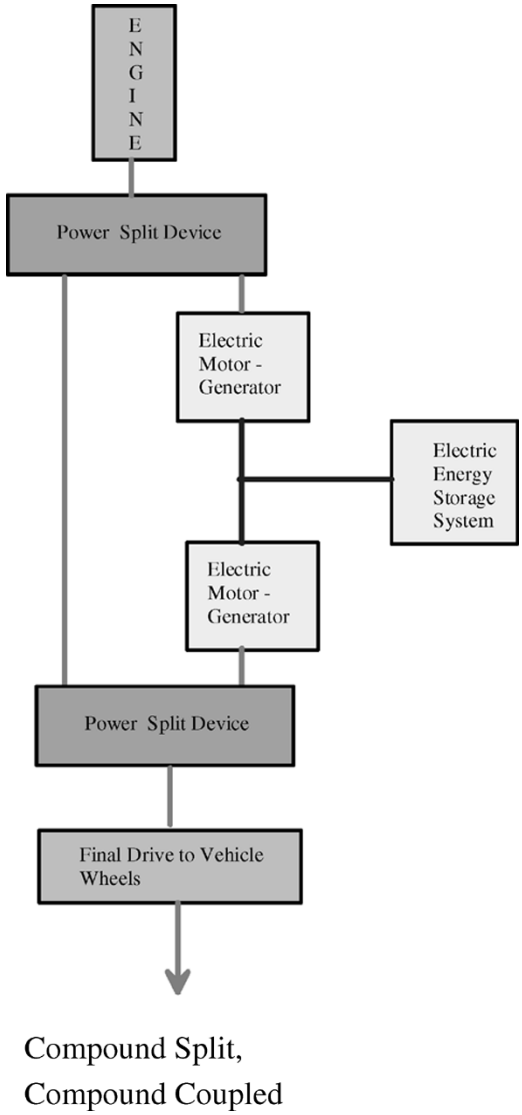

Fig. 4. Compound split e-CVT architecture.

C. Power Split Device of the e-CVT

The planetary gear set is the core of the power split transmission and the means through which engine torque splits, a portion to the generator and a portion to the driveline. Fig. 5 is a schematic of a planetary gear having four planets supported by a carrier and interposed between the central sun gear and outer ring gear (i.e., internal gear).

The fundamental equation of the planetary gear (i.e., epicyclic gearing) is that the gear rotation must maintain a fixed ratio of angular velocity relative to the carrier body. This fixed ratio is defined as the basic ratio, k, and it equals the radius (or number of teeth) of the ring divided by the radius (or number of teeth) of the sun gear. The basic ratio of the planetary gear, power split device follows:

$$\frac{\omega_s - \omega_c}{\omega_r - \omega_c} = -\frac{r_r r_p}{r_p r_s} = -\frac{r_r}{r_s} = -k. \tag{1}$$

After simplification, (1) reduces to the more general form, (2) which illustrates the inherent speed summing nature of the planetary gear and the reason it is used in power split

$$\omega_s + k\omega_r - (k+1)\omega_c = 0. \tag{2}$$

Alternatively, (1) can be written in terms of its gear radii as

$$\omega_c = \frac{r_s}{2r_c}\omega_s + \frac{r_r}{2r_c}\omega_r. \tag{3}$$

With this introduction to power split e-CVTs the two basic systems are discussed in more detail in Section II for the input split and Section III for the compound split. Section IV extends the treatment of compound split to include two-mode variants as developed by Timken and Renault. Some discussion of the series-parallel switching architecture is given in Section V.

II. Dynamics of the Input Split e-CVT

The input split architecture as developed by Toyota Motor Co. is now used in the Prius sedan, the RX400H, and Highlander sport utility vehicles (SUVs), and in 2006 its Harrier and Kluger SUVs in Japan. The input split is analyzed by first sketching out the implementation, second, ascribing to each occurrence of a gear set a direction and magnitude for the described ratio, and third, assigning magnitudes to all inertias. In this paper, gear

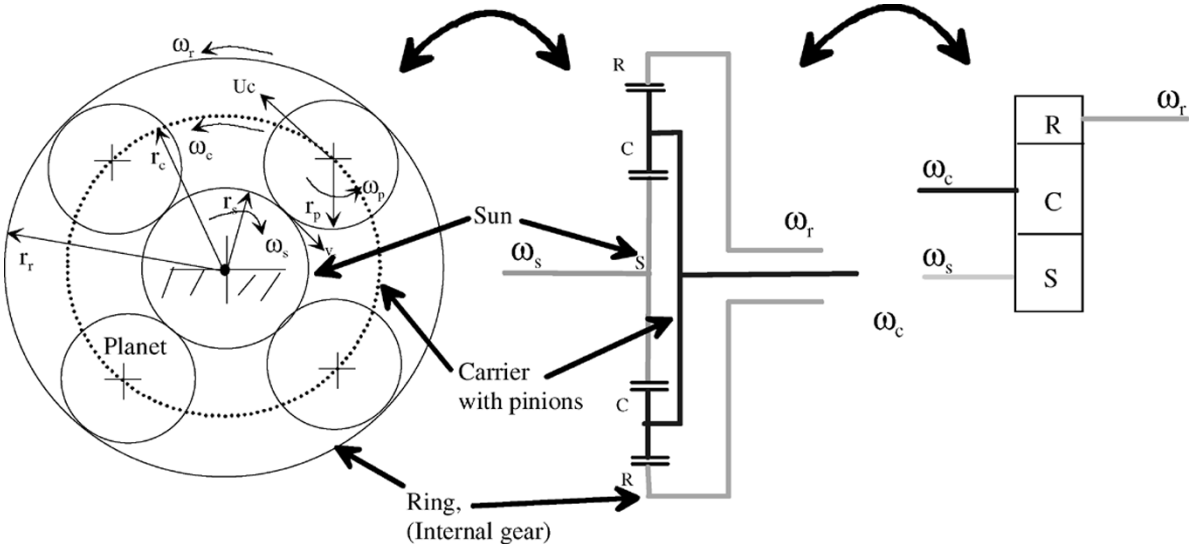

Fig. 5. Description of the power split device.

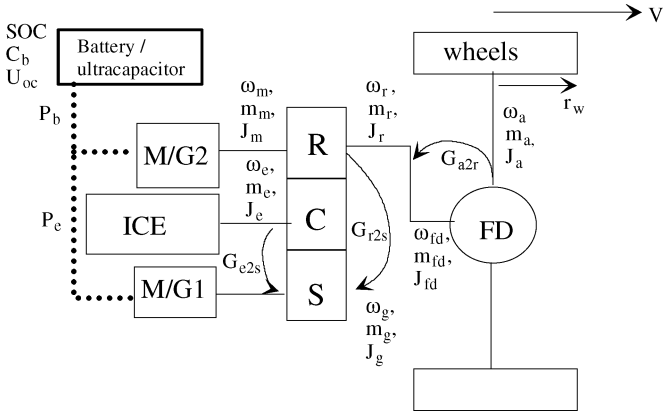

Fig. 6. Toyota Hybrid System (THS)-I & II input split e-CVT.

mesh and component inefficiency are not treated, but can be included by simply attaching an efficiency value to each occurrence of a torque translation in the schematic at the arrow tip side.

A. Toyota's Hybrid System (THS) (I & II)

Fig. 6 illustrates the architecture of the THS propulsion system, an input coupled, single planetary stage with dual electric machine implementation. All gear ratios are assigned, inertias of interest identified, and physical variables noted.

Details of the THS power split system dynamics can be found in [2]–[4] with additional technical background in [5]–[7]. Fig. 1 is the complete system level functional diagram of the THS power split hybrid propulsion system including electronic throttle control (ETC) for engine torque management, regenerative brake system (RBS) for electronic management of the vehicle brakes, as well as energy management system (EMS) control of the energy storage system (ESS).

The angular speed, ω, torque, m, and inertia, J, variables used in this paper are identified by subscripts: a = axle, fd = final drive, m = motor, r = ring (also known as the internal gear). Descriptions of the lumped inertia terms are given in the Appendix. The input split model of Fig. 6 is analyzed in detail in [4], and for which the salient dynamics presented to the generator, M/G1, the engine, ICE, and the traction motor-generator, M/G2, are described as follows. The generator shaft torque becomes

$$m_g = \frac{1}{G_{e2s}}\{m_e - J_e\dot{\omega}_e - J_{gc}\dot{\omega}_m\}. \tag{4}$$

The overall expression for THS driveline torque, including all dynamic effects, at the power summation point is given as

$$m_r = m_m - \frac{G_{r2s}}{G_{e2s}}m_e + \left(\frac{G_{r2s}}{G_{e2s}}J_{eq} - J_{gc}\right)\dot{\omega}_e + \left(\frac{G_{r2s}}{G_{e2s}}J_{gc} - J_{mq}\right)\dot{\omega}_m \tag{5}$$

where (5) is the fundamental relationship for propulsion torque in the input split transmission, e-CVT, and moreover, (5) must equal the road load resisting torque given in (6), m'_{r}, where the resisting torque reflected to the driveline, m'_{r} is expressed as

$$m'_r = \frac{r_w}{G_{a2r}}F_{\mathrm{road}} + (M_v + M_{\mathrm{Pass}})\frac{dV}{dt}. \tag{6}$$

In (6), vehicle rolling resistance and aerodynamic drag are lumped in parameter F_{road} with acceleration of all masses contained in the second term. Rewriting (6) for the steady-state condition (highway cruise) highlights the input split torque partitions without dynamics. The steady-state (cruise mode) propulsion torque is then

$$\begin{aligned} m_{rss} &= m_m - \frac{G_{r2s}}{G_{e2s}}m_e \\ G_{r2s} &= -k \\ G_{e2s} &= (k+1). \end{aligned} \tag{7}$$

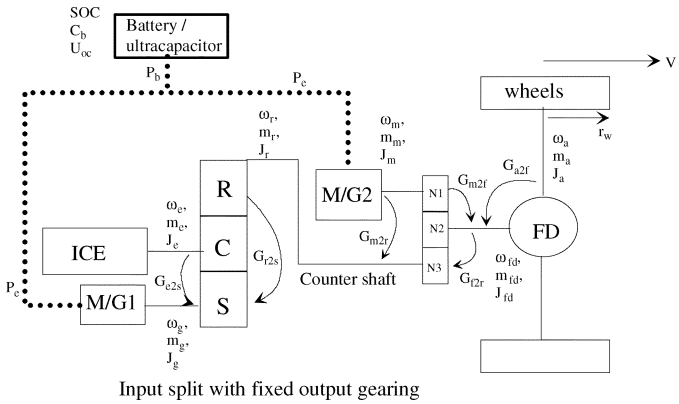

Fig. 7. Ford Hybrid System, FHS, input split e-CVT.

Substituting for the gear ratios as defined in (7) the driveline steady state torque is given as the second expression in (8). Similarly, the generator torque with dynamics (4) reduces to the top expression in

$$m_{gss} = \frac{1}{k+1} m_e$$
$$m_{rss} = m_m + \frac{k}{k+1} m_e. \tag{8}$$

B. Ford Hybrid System, FHS, an Input Split e-CVT

The architecture of the Ford e-CVT is shown as Fig. 7 where the input split character of the THS is retained but coupled with an output torque multiplier stage in the form of spur gears.

The input split with output torque multiplier model of Fig. 7 is analyzed in detail in [4], further background can be found in [8]. The salient dynamics presented to the generator (M/G1) the engine (ICE) and the traction motor-generator, (M/G2) are described below. Description of the lumped inertia's are given in the Appendix. The generator shaft torque becomes

$$m_g = \frac{1}{G_{e2s}} \{ m_e - J_{eq} \dot{\omega}_e - J_{gc} \dot{\omega}_m \}. \tag{9}$$

Overall driveline torque in the FHS configuration, again including all dynamic effects is taken at the input to the final drive (FD). The dynamic expression for FHS configuration final drive torque is similar to (5) but with more complexity in the scaling constants due to output gearing (term $G_{\rm cs}$). For FHS the driveline torque is:

$$m_{fd} = \frac{1}{G_{m2f}} m_m - G_{cs} m_e + \left(G_{cs} J_{eq} - \frac{1}{G_{a2f}} J_{gc} \right) \dot{\omega}_e + \left(G_{cs} J_{gc} - \frac{1}{G_{a2f}} J_{mq} \right) \dot{\omega}_m. \tag{10}$$

The developed torque of (10) must balance the road load torque reflected up the driveline to the final drive input. In the steady state, i.e., highway cruise, the driveline torque is

$$m_{fdss} = \frac{1}{G_{m2f}} m_m - G_{cs} m_e. \tag{11}$$

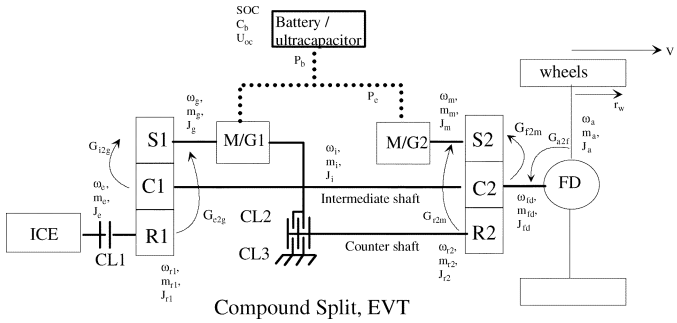

Fig. 8. GM–Allison compound split e-CVT, a two-mode transmission.

Making the ratio substitutions using the definitions in the Appendix, the steady-state driveline torque of the FHS type input split system is

$$m_{fdss} = \left(\frac{N_2}{N_1} \right) m_m + \left(\frac{k}{k+1} \right) \left(\frac{N_2}{N_3} \right) m_e. \tag{12}$$

The input split e-CVTs have a characteristic driveline torque composed of a specified fraction of the available engine torque and either a unity ratio on traction motor torque, THS architecture, or torque multiplied effect of the traction motor, FHS architecture. In the next section, it will be shown that when the output gearing of an FHS type e-CVT is replaced with a second power split device that a new type of e-CVT is realized having the properties of input split in one (city) mode and the flexibility of input and output differentials in a second (highway) mode. This is the compound split system developed originally by Allison for GM as a hybrid bus and heavy vehicle transmission.

III. Dynamics of the Compound Split e-CVT

The compound split system is distinctly different from the input split e-CVT in that it is capable of variable structure control. The structure modifying elements being the inclusion of mechanical disconnect clutches and in some systems the incorporation of hydraulic brakes. Clutch packs are typically expensive transmission components when slippage is required, i.e., a drive clutch. However, simple disconnect clutches are inexpensive and akin to hydromechanical brakes. Fig. 8 is the architecture of the Allison hybrid bus compound split transmission [9], now referred to as a two-mode.

The two-mode e-CVT is similar in many respects to the FHS input split system with output gearing. Only, in the GM two-mode system the output gear is a planetary gear set. Geared neutral is available by disengaging both clutches 2 and 3. The two-mode is also known as an electric variable transmission (EVT). The two-mode can be analyzed by considering each of its modes separately.

A. Compound Split, GM Two-Mode in Low Range

Low range, mode 1 in the compound split e-CVT is entered when clutches $\mathrm{CL1} = 1$, $\mathrm{CL2} = 0$, $\mathrm{CL3} = 1$ and the system becomes input split in operation. In this mode, as with THS and FHS before, $\mathrm{M/G1} =$ generator and $\mathrm{M/G2} =$ motor. This is shown in Fig. 9 where planetary set E1 operates as a differential

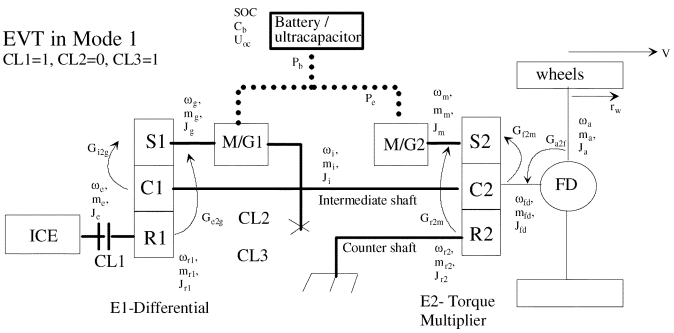

Fig. 9. GM–Allison EVT, in mode 1—low range.

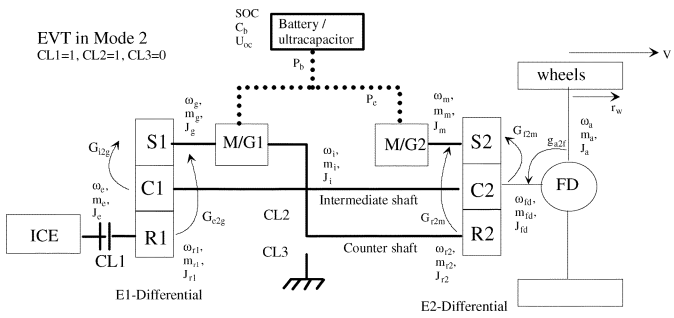

Fig. 10. GM–Allison EVT, in mode 2—high range.

and set E2 as a torque multiplier. Fig. 9 is the same as Fig. 8 but with the clutches activated.

Dynamics of the EVT in mode-1 for city driving reveal that the generator, M/G1, torque is consistent with (9) for the FHS system as given in (13) with all inertia parameters identified in the Appendix. In fact, with the ring gear of E2 grounded by clutch CL3 the compound split EVT in mode 1 inherently contains most elements of the input split with output gearing. E2 is in fact a torque multiplier in this mode

$$m_g = \frac{1}{G_{e2g}}\{m_e - J_{eq}\dot{\omega}_e - J_{gc}\dot{\omega}_m\}. \tag{13}$$

Carrying out the derivation of compound split driveline torque into the final drive $m_{\rm fd}$, results in

$$m_{fd} = G_{f2m}m_m - \frac{G_{i2g}}{G_{e2g}}m_e + \left(\frac{G_{i2g}}{G_{e2g}}J_{eq} - G_{f2m}J_{gc}\right)\dot{\omega}_e + \left(\frac{G_{i2g}}{G_{e2g}}J_{gc} - G_{f2m}J_{mq}\right)\dot{\omega}_m. \tag{14}$$

The similarity of (14) to (10) is striking and consistent with the compound split having E1 in differential mode, i.e., input split and E2 in torque multiplier mode, i.e., output gearing. In steady-state the generator torque (13) and driveline torque (14) reduce to

$$\begin{aligned} m_{gss} &= \frac{1}{G_{e2g}}m_e \\ m_{fdss} &= G_{f2m}m_m - \frac{G_{i2g}}{G_{e2g}}m_e. \end{aligned} \tag{15}$$

Substituting for the ratios according to the definitions given in the Appendix reduces (15) to a more insightful form

$$\begin{aligned} m_{gss} &= \frac{-1}{k^{E1}}m_e \\ m_{fdss} &= (k^{E1}+1)m_m + \left(\frac{k^{E1}+1}{k^{E1}}\right)m_e. \end{aligned} \tag{16}$$

Which is the motor and engine torque combination according to input split conditions. Planetary gear basic ratio, k, is superscripted to reflect its association with the input, E1, or output, E2, power split device, respectively.

B. Compound Split, GM 2-Mode in High Range

High range, mode 2 in the compound split e-CVT is entered when clutches $\mathrm{CL1} = 1$, $\mathrm{CL2} = 1$, $\mathrm{CL3} = 0$ and the system operates as both input and output split, hence, compound split. In the high range, or highway mode, the e-CVT is capable of negotiating grades, towing, and sustained cruise. In mode-2 both planetary sets, E1 and E2 operate as differentials. Fig. 10 is the same as Fig. 8 but with the appropriate clutches activated. The EVT under mode-2 control is true input and output split. It is also noteworthy that compound split e-CVTs, as a general rule of four-ports, have their M/Gs associated with planetary set sun gears.

Operation under mode 2 for the EVT results in generator, M/G1, torque that is consistent with earlier derivations, and in fact, its steady-state value is identical to that given by (16)

$$\begin{aligned} m_g &= \frac{1}{G_{e2g}}\{m_e - J_{eq}\dot{\omega}_e - J_{gc}\dot{\omega}_m\} \\ m_{gss} &= \frac{1}{G_{e2g}}m_e = \frac{-1}{k^{E1}}m_e. \end{aligned} \tag{17}$$

EVT output torque to the final drive, i.e., driveline torque under mode-2 is significantly different from mode 1 as given in (14) and (15). In this case

$$m_{fd} = \frac{1}{G_{f2m}}m_m - \frac{1}{G_{f2m}G_{r2m}G_{e2g}}m_e + \frac{1}{G_{f2m}}J_{eq2}\dot{\omega}_e - \frac{1}{G_{f2m}}J_{mq}\dot{\omega}_m. \tag{18}$$

The highway cruise driveline torque under mode two is found by setting the derivatives in (18) equal to zero. In this case, the steady-state driveline torque into the final drive is

$$\begin{aligned} m_{fdss} &= \frac{1}{G_{f2m}}m_m - \frac{1}{G_{f2m}G_{r2m}G_{e2g}}m_e \\ m_{fdss} &= \frac{1}{k^{E2}+1}m_m - \frac{1}{(k^{E2}+1)(-k^{E2})(-k^{E1})}m_e. \end{aligned} \tag{19}$$

Comparing (19) to the bottom equation in (16) it is apparent that driveline torques in mode 1 and mode 2 are very different. Furthermore, the driveline torque of the compound split system during mode 2 contains elements of both planetary gear sets acting as differentials.

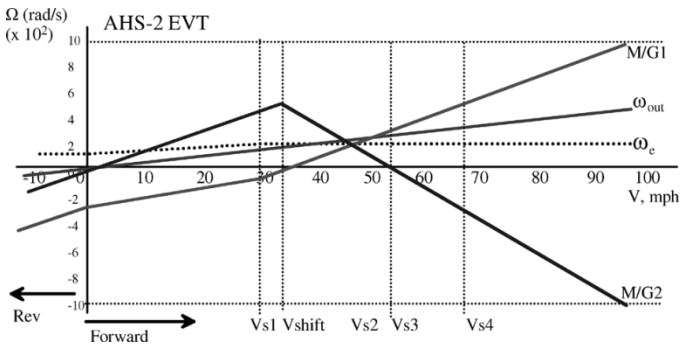

Fig. 11. GM–Allison EVT ac drive system operation.

C. Compound Split Operation Over Full Vehicle Speed Range

To complete this coverage of compound split it is necessary to consider how the EVT ac drive systems function. As in all power split architectures, one port of the power split device must provide a reaction torque to enable the mechanical transfer of power between the remaining two ports. To illustrate the presence of two mechanical nodes a plot of motor-generator speed is developed given vehicle operation from reverse to top end speed. Fig. 11 illustrates the direction and magnitude of both M/G1 and M/G2 of the EVT under this type of operation.

In Fig. 11, the vehicle engine speed is assumed to ramp from 180 rad/s at vehicle standstill (and reverse) to 240 rad/s. Engine speed increases with vehicle speed until vehicle speed, Vs1, is reached, after which the engine speed remains steady. The EVT output angular speed, $\omega_{\rm o}$, tracks the vehicle speed from reverse through stopped and up to maximum speed. M/G2, the ac drive system at the output differential, E2, tracks vehicle speed during mode 1 operation (e.g., vehicle speed is less than $V_{\rm shift}$). The speed designated $V_{\rm shift}$ occurs when ac drive system, M/G1, reduces its angular speed to zero. This is the first mechanical node and the point at which clutch actuation occurs. Under this synchronous shift, the speed of traction motor, M/G2 begins to fall until it reaches zero. When the angular speed of M/G1 reaches zero the EVT has encountered its second mechanical node. Above the second node, both ac drive systems increase in speed consistent with vehicle speed and the particular engine operating strategy.

IV. Variants of Compound Split e-CVTs

There are now two variants of the original GM–Allison compound split system under development. In this paper, these systems will be referred to as the eVT, or electromechanical infinitely variable transmission as developed by Timken [10] and the infinitely variable transmission, IVT, as developed by Renault [11], respectively.

A. Compound Split, Timken, eVT Type

The eVT is shown schematically in Fig. 12 in the conventional transmission line drawing fashion of being symmetric about its centerline. This provides the designer with insight into how the various concentric shafts must be routed, and more importantly, where the bearings must be located. The e-CVT is a four-port with input, ICE, and output to final drive ports on the left and variator input, $\omega_{\rm vi}$, and output, $\omega_{\rm vo}$, ports on the right.

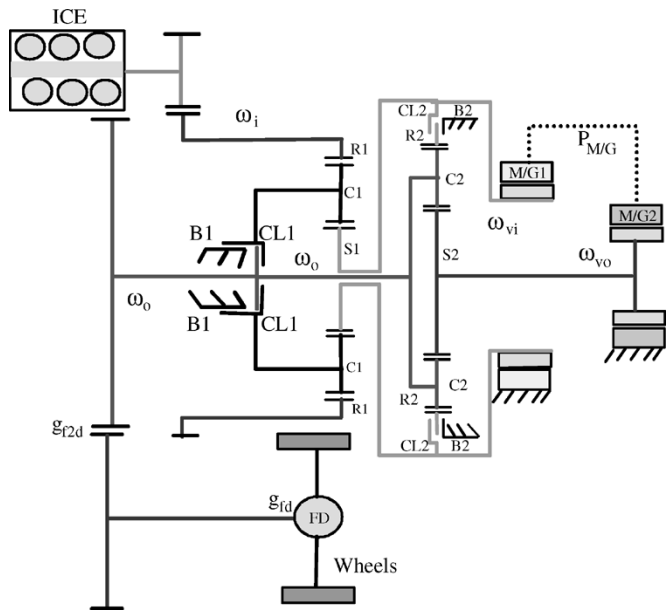

Fig. 12. Timken eVT full line schematic.

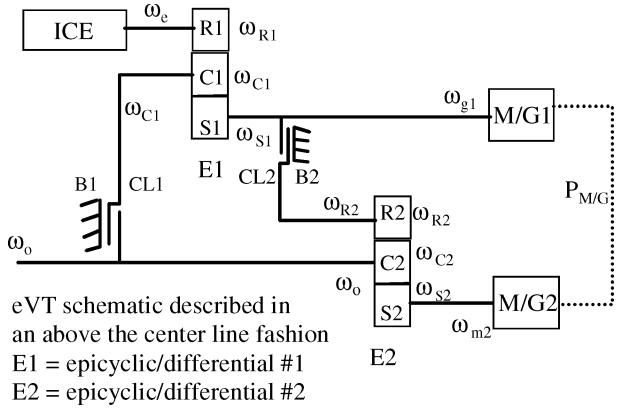

Fig. 13. Timken eVT after reduction by symmetry.

The design is fully take-apart. The angular speeds at these ports are found by application of (2) to planetary sets E1 and E2 in Fig. 12 and perhaps more readily from Fig. 13

$$\begin{aligned}\omega_{g1}+k^{E1}\omega_0&=(k^{E1}+1)\omega_e\\ \omega_{m2}+k^{E2}\omega'_{g1}&=(k^{E2}+1)\omega_0.\end{aligned}\tag{20}$$

The usual convention in transmission schematic development is to cut the transmission line diagram, here Fig. 12, at the centerline and redraw only the top half recognizing that by symmetry the full transmission is shown. This is done with Fig. 12 and after rearrangement and using the graphic for planetary sets the functional diagram of Fig. 13 results.

As there are no gear shifts nor drive clutches to control in e-CVTs such systems must provide all the automatic transmission functions customers are accustomed to. These functions are represented by the shift level PRNDL display which depicts Park, Reverse, Neutral, Drive, and Low. All the e-CVTs provide these functions, but the control is simply a digital command rather than an actual lever position. In the eVT of Figs. 12 and

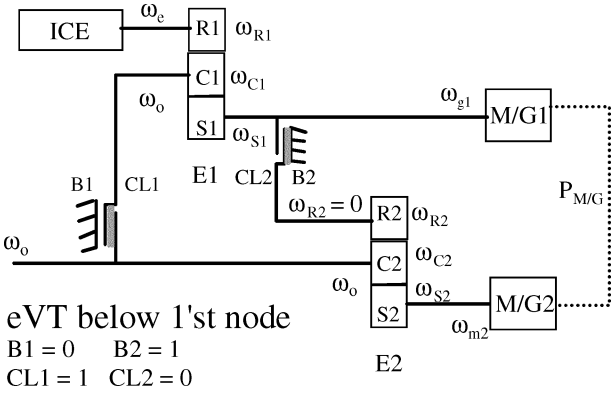

Fig. 14. Timken eVT clutch and brake control below first node.

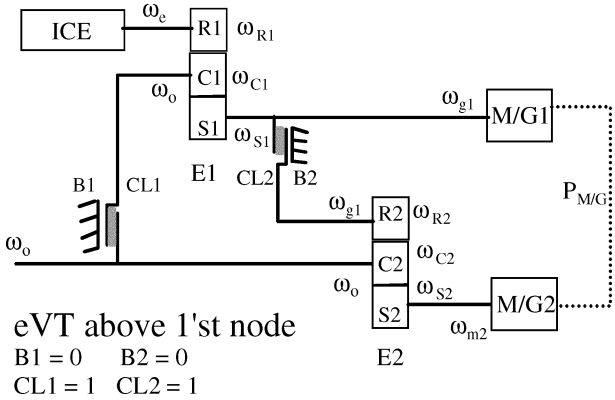

Fig. 15. Timken eVT clutch and brake control above first node.

13, the activation of disconnect clutches and hydraulic brakes are used to engage each function as follows.

- Parked and braking: $\mathrm{CL1}=1, \mathrm{CL2}=0, \mathrm{B1}=1, \mathrm{B2}=0$.
- Reverse: $\mathrm{CL1}=0, \mathrm{CL2}=0, \mathrm{B1}=1, \mathrm{B2}=1$.
- Geared neutral: M/G1 freewheels and M/G2 is locked.
- Drive modes are described in the next section.

B. Compound Split, eVT Type, Operation Below First Node

To describe this operational region of the eVT it is necessary to employ a theory of variators to identify when the mechanical nodes occur. The first mechanical node of the eVT occurs when the variator ratio $K_{\mathrm{v}}(K)=0$. Vehicle speed from launch up to the first mechanical node is controlled as shown in Fig. 14 where $\mathrm{CL1}=1$ and $\mathrm{B2}=1$, i.e., are engaged.

Transmission mechanical port variables ω_0 and ω_{e} in (20) are solved in the form of ratios, $K=\omega_0/\omega_{\mathrm{e}}$, and the variator, $K_{\mathrm{v}}=\omega_{\mathrm{v0}}/\omega_{\mathrm{vi}}=\omega_{\mathrm{m2}}/\omega_{\mathrm{g1}}$, where the following definitions apply:

$$\begin{aligned}\alpha_1&=\frac{1}{k^{E1}+1};\ldots\ldots\beta_1=\frac{k^{E1}}{k^{E1}+1}\\ \alpha_2&=\frac{1}{k^{E2}+1};\ldots\ldots\beta_2=\frac{k^{E2}}{k^{E2}+1}.\end{aligned}\tag{21}$$

Manipulating (20) and using (21) results in an expression for transmission ratio, K, below the first node which is identified as K_{-1} [10]

$$K_{-1}(K_v)=\frac{\alpha_2 K_v}{\alpha_1+\beta_1\alpha_2 K_v}.\tag{22}$$

As the next step (22) is solved for K_{v} to determine the node points, one of which is $K_{\mathrm{v}}=0$ which results in $K_{-1}=0$ to signify a stopped or parked vehicle. The second zero point is when $(1/K_{\mathrm{v}})=0$ or

$$\begin{aligned}&K_v=\frac{\alpha_1 K_{-1}}{\alpha_2-\beta_1\alpha_2 K_{-1}}=0\\ &\therefore\ K_{-1}=0\ldots\ldots Vehicle.stopped\\ &\frac{1}{K_v}=0\\ &\therefore\ K_{-1}=\frac{\alpha_2}{\beta_1\alpha_2}=\frac{k^{E1}+1}{k^{E1}}.\end{aligned}\tag{23}$$

In (23), the vehicle speed at which the first node occurs is completely determined by the planetary gear E1 characteristics. This is a very fundamental property of e-CVTs and it applies in general.

C. Compound Split, eVT Type, Operation Above First Node

At the first mechanical point identified in (23) both brakes are released and both clutches activated as depicted in Fig. 15. Employing the same procedure as used in Section IV-B, above, the transmission ratio is now

$$K_{+1}(K_v)=\frac{\beta_2+\alpha_2 K_v}{\left[\frac{\alpha_1}{\alpha_1-1}+\frac{\beta_2}{\beta_1}\right]+\frac{\alpha_2}{\beta_1}K_v}.\tag{24}$$

Solving (24) for K_{v} and setting this expression equal to zero results in

$$K_{+1}=\frac{\beta_1\beta_2}{\left(\frac{\alpha_1\beta_1}{\alpha_1-1}+\beta_2\right)}=\frac{k^{E1}k^{E2}}{k^{E1}k^{E2}-1}.\tag{25}$$

In (25), the planetary sets E1 and E2 are both acting as differentials with the result that the second node occurs at a vehicle speed dependent on the selection of the basic ratios of E1 and E2.

What is interesting in the eVT, and in all e-CVTs for that matter, is to determine the transmission ratio spread, $\mathrm{K}_{+1}-\mathrm{K}_{-1}$, between the mechanical nodes. This measure is related to conventional transmission gear shift ratio coverage, an important metric of driveability. In the eVT (24) and (25) predict the ratio spread given by (26) assuming for convenience that both E1 and E2 have the same basic ratio

$$K_{+1}-K_{-1}=\frac{k(k+1)}{(k^2-1)(k+1)}=\frac{k}{(k^2-1)}.\tag{26}$$

The insightful reader will recognize from (26) that the eVT configuration will only obtain wide transmission ratio coverage provided the planetary gear set basic ratio is selected as close as possible to 1.5. According to (3) a basic ratio, $k=1.5$ means that the planet gears on the carrier would need to have a radius $r_{\mathrm{p}}=1/4$ that of the sun gear r_{s}.

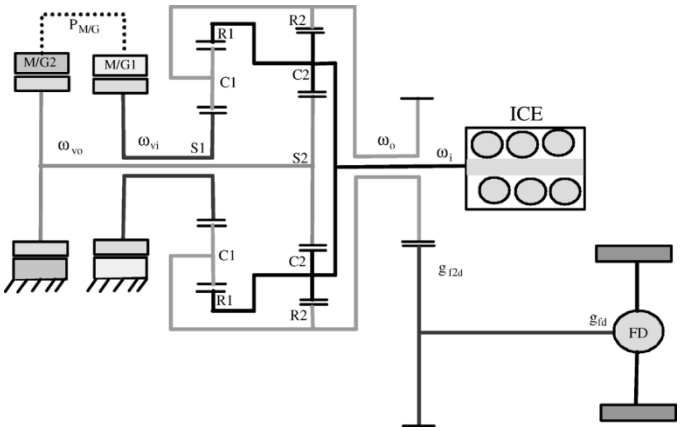

Fig. 16. Renault IVT full line schematic.

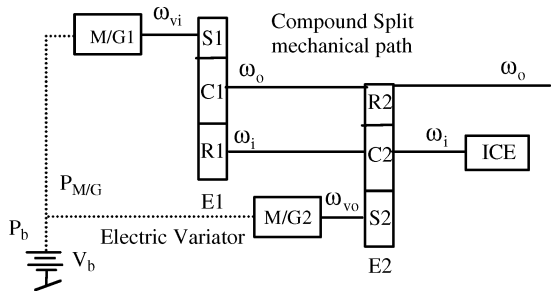

Fig. 17. Renault IVT reduction by symmetry.

D. Compound Split, Renault, IVT Type

The architecture of the IVT is shown as a full function schematic in Fig. 16. This again is a four-port arrangement.

As a four-port electromechanical system having two-mechanical only ports and two-electromechanical ports the IVT will be analyzed following the method of (20) with the same definitions (21) applied to E1 and E2 in the functional diagram of Fig. 17. In this case, (20) becomes

$$\begin{aligned}(1-\beta_1\beta_2)\omega_i &= \alpha_1\beta_2\omega_{vi}+\alpha_2\omega_{v0}\\ (1-\beta_1\beta_2)\omega_0 &= \alpha_1\omega_{vi}+\beta_1\alpha_2\omega_{v0}.\end{aligned} \tag{27}$$

The IVT system has an electric-variator response typical of all compound split systems as can be seen from inspection of (28) and comparing with (23)

$$\begin{aligned}K_v &= \frac{\alpha_1\beta_2K-\alpha_1}{\beta_1\alpha_2-\alpha_2K}\\ K_{v1}|_{\omega_{vi}=0} &= \beta_1 = \frac{k^{E1}}{k^{E1}+1}\\ K_{v2}|_{\omega_{v0}=0} &= \frac{1}{\beta_2} = \frac{k^{E2}+1}{k^{E2}}.\end{aligned} \tag{28}$$

The corresponding mechanical nodes for the IVT are found by substituting (28) into (29) and computing the transmission ratio that results. In the IVT the transmission function becomes

$$K = \frac{\frac{\alpha_1}{\alpha_2}+\beta_1K_v}{\frac{\alpha_1}{\alpha_2}\beta_2+K_v}. \tag{29}$$

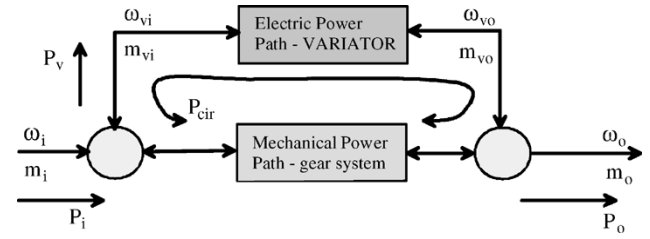

Fig. 18. Power flows in the electromechanical four-port system.

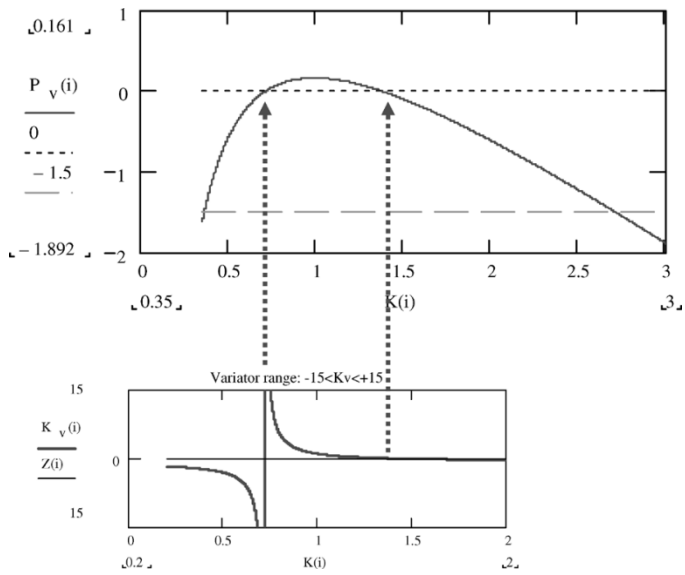

Fig. 19. Variator power fraction in the IVT.

Of interest is the fact that the IVT has variator nodes (28) located at $K_{\rm v1}=0.73$, $K_{\rm v2}=1.4$ when $k^{\rm E1}=2.7$ and $k^{\rm E2}=2.5$. The IVT admits $k\sim 2.6$ for nominal response.

Power flow in the electric variator can be understood by referring to Fig. 18. In this figure, electric path power Pv is used to control mechanical path power.

In Fig. 18, the electric path variator power is defined as (30) and after plotting versus transmission ratio K in Fig. 19 shows the relationship of variator zeros to mechanical nodes

$$P_v = \frac{m_{vi}\omega_{vi}}{m_i\omega_i} = \frac{\beta_2K+\beta_1-(\beta_1\beta_2-1)K}{(\beta_1\beta_2-1)K}. \tag{30}$$

Fig. 19 reveals that electric power flow in the variator between the mechanical nodes is very modest, approximately 0.25 pu of the throughput power. Second, the roots of the variator expression identify the transmission nodes. Using this analytical procedure it can be seen that e-CVTs of the compound type having a wide spread in variator roots are desirable from the standpoint of high equivalent gear shift ratio coverage and moderate to low electric path power requirements.

V. Series Parallel Switching Type

The final architectural type to be considered is the series-parallel switching configuration. This propulsion architecture is important because it requires a single ac drive system versus dual ac drives that are needed in all power split systems. Second, the series-parallel switching configuration is amenable to rear

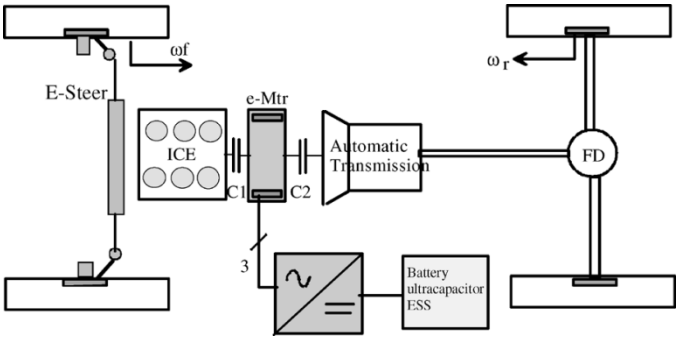

Fig. 20. Series-parallel switching architecture.

wheel drive vehicles. Power split types are most often, if not universally, applied to front wheel drive vehicles. Fig. 20 illustrates the series-parallel switching architecture configured for rear wheel drive vehicles as it was described in 2002 by the Toyota Motor Co.

In addition, the series-parallel architecture admits wide latitude of M/G power levels so that mild and full hybridization is possible. The series-parallel switching architecture can therefore be used as either a power assist hybrid or as a dual mode hybrid. The distinction determined by the capacity of its electric ESS (i.e., dual mode equals plug-in hybrid).

Power train coordination in the series-parallel switching configuration is less complex than in power split because only two, rather than three, independent torque sources are being managed. In the configuration of Fig. 20, clutch C1 is a disconnect device such as those used in the compound split architectures. Clutch C2 is the drive clutch and it must be designed for slippage. The transmission may be a manual, automatic with torque converter or a mechanical CVT. From a cost and complexity perspective this configuration is better suited to automotive applications than power split, but it will not have the smooth and seamless torque transmission properties of the power split.

The series-parallel switching architecture has the potential to be introduced by one of the major automotive companies in the near term. This would make an excellent propulsion system for rear wheel drive full size sedans. Today, the power split system is used on the front axle and a separate electric drive is used on the rear axle as the means of introducing on demand four wheel drive such as Toyota's E-Four system.

VI. Conclusion

This paper has explored the various types of power split e-CVTs now used or being planned for near term use. The e-CVT, as such systems are generically known, offer smooth and seamless driveability during all modes of operation. The e-CVT is also more efficient than mechanical CVTs, especially as the transmission ratio coverage approaches 6:1. This paper has developed the dynamics of the e-CVT and has shown the similarity of the various types and their major differences. In particular, the compound split in mode 1 was shown to contain most of the elements of the input split system. The compound split in mode 2 was shown to constrain the operating speed range of the ac drives used and therefore to hold out the possibility of using asynchronous electric machines in place of the interior permanent magnet machine demanded by input split systems. Because of fixed gearing in single mode systems there is an inevitable need for very wide constant power speed range ac drives if the vehicle is to operate over reasonable automotive speeds. In conclusion, the power flow through the electric variator was developed and illustrated graphically. Last, the series-parallel switching configuration was shown as a promising hybrid propulsion architecture that requires a single ac drive subsystem rather than the dual ac drives required in all power split transmissions.

Appendix

The lumped parameter variables used in the e-CVT architectures are listed here for reference. All gear ratios are shown as $G_{\mathrm{start2finish}}$ in the figures and equations. Start defines the origin of the effort variable, m, as in $m_{\mathrm{e}} = G_{\mathrm{e2g}} m_{\mathrm{g}}$ and just the reverse for the flow variable, ω as in $\omega_{\mathrm{g}} = G_{\mathrm{e2g}} \omega_{\mathrm{e}}$. The convection with reflected inertias follows the same convection as the effort variable. In the THS system lumped inertias included in the expressions of dynamics are obtained from the following derivations. First, reflecting the axle shaft inertia J_{a} to the driveline, or final drive input as J_{fd} results in (A1) where a term is included to capture the final drive shaft inertia

$$J_{fd} = \frac{1}{G_{a2r}^2} J_a + J_{fd\_sh}. \tag{A1}$$

The same procedure applies to the traction motor shaft, M/G2 at which the motor rotor inertia itself is present as J_{mot}, in addition to the inertia of the ring gear, J_{r}, and the reflected inertia on the final drive (A1) and sun gear inertia, J_{s}, plus generator rotor inertia, J_{g}, all reflected to the motor shaft

$$\begin{aligned} J_m &= J_{mot} + J_r + J_{fd} + G_{r2s}^2 (J_s + J_g) \\ J_g' &= (J_s + J_g). \end{aligned} \tag{A2}$$

At the engine shaft the resulting lumped inertia is due to the engine crank, Jcrank, planetary set carrier with planet gears, and the sun and generator rotor inertias reflected to the engine shaft via the carrier to sun ratio

$$J_e = J_{\mathrm{crank}} + J_c + G_{e2s}^2 J_g'. \tag{A3}$$

When the planetary gear speed relation is introduced into the engine and traction motor dynamics a new inertia term is introduced at both the traction motor and engine shafts. This generator couple consists of the reflected inertia of the generator inertia plus the sun gear inertia. Note that in the convention used the planetary ring to sun ratio is defined as $-k$

$$\begin{aligned} G_{e2s} &= (k+1) \\ G_{r2s} &= -k \\ \omega_g &= G_{e2s} \omega_e + G_{r2s} \omega_r. \end{aligned} \tag{A4}$$

The remaining lumped inertia terms for the THS system are

$$\begin{aligned} J_{gc} &= G_{e2s} G_{r2s} (J_g + J_s) \\ J_{eq} &= J_e + G_{e2s}^2 J_g' \\ J_{mq} &= J_m + G_{r2s}^2 J_g'. \end{aligned} \tag{A5}$$

In the FHS system, the definitions of (A4) apply, but due to the output gearing at the traction motor, or torque multiplier, the expressions (A2) and (A3) must be modified and some new definitions applied. At the geared output the new ratios are

$$\begin{aligned} G_{m2r} &= \frac{N_1}{N_3} \\ G_{m2f} &= \frac{N_1}{N_2} \\ G_{f2r} &= \frac{N_2}{N_3} \\ G_{a2f} &= \frac{N_5}{N_4}. \end{aligned} \tag{A6}$$

Next, the traction motor, engine, and generator couple inertias are defined for the FHS architecture

$$\begin{aligned} J_{m\_sh} &= J_{mot} + G_{m2r}^2 J_r + G_{m2f}^2 J_{fd} + \frac{G_{m2f}}{G_{a2f}} J_a \\ J_m &= J_{m\_sh} + G_{m2r} G_{r2s} J_g' \\ J_e &= J_{\text{crank}} + J_c + G_{e2s}^2 J_g'. \end{aligned} \tag{A7}$$

After a similar derivation of the engine and traction motor dynamics a generator couple is defined that lumps the generator inertia's on each of these shafts and it is

$$J_{gc} = G_{m2r} G_{r2s} G_{e2s} J_g'. \tag{A8}$$

Similar to (A5) engine and traction motor equivalent inertia's are computed

$$\begin{aligned} J_{mq} &= J_m + G_{m2r}^2 G_{r2s}^2 J_g' \\ J_{eq} &= J_e + G_{e2s}^2 J_g'. \end{aligned} \tag{A9}$$

Last, for the output torque multiplier effect of the FHS configuration a new ratio term must be defined that translates engine torque to the final drive

$$G_{cs} = \frac{G_{m2r} G_{r2s}}{G_{m2f} G_{e2s}}. \tag{A10}$$

In the GM-Allison system, two-mode or EVT, a new set of gear ratios must be defined. First, for E1

$$\begin{aligned} G_{e2g} &= -k^{E1} \\ G_{i2g} &= k^{E1} + 1. \end{aligned} \tag{A11}$$

And for planetary set E2

$$\begin{aligned} G_{f2m} &= k^{E2} + 1 \\ G_{r2m} &= -k^{E2} \\ G_{a2f} &= \frac{N_5}{N_4}. \end{aligned} \tag{A12}$$

In (A12), the axle to final drive ratio is given to be consistent with the FHS configuration. The inertias in the GM 2-mode system are

$$\begin{aligned} J_e &= J_{\text{crank}} + J_{R1} + G_{e2g}^2 (J_s + J_{mg1}) \\ J_{mot\_sh} &= J_{mg2} + J_{S2} + \frac{1}{G_{f2m}^2} \left(J_{fd} + \frac{1}{G_{a2f}^2} J_a \right) \\ J_i &= J_{C1} + G_{i2g}^2 (J_s + J_{mg1}) \\ J_m &= J_{mot\_sh} + \frac{1}{G_{f2m}^2} J_i. \end{aligned} \tag{A13}$$

The angular speeds at E1 and E2 are

$$\begin{aligned} \omega_{g1} &= G_{i2g} \omega_i + G_{e2g} \omega_e \\ \omega_m &= G_{f2m} \omega_{fd} + G_{r2m} \omega_{r2}. \end{aligned} \tag{A14}$$

In the dynamic expressions for the two-mode EVT the following lumped inertias are defined. (A15) lists the equivalent inertia at the engine shaft, J_{eq}, the generator couple, J_{gc}, and at the motor M/G2 shaft J_{mq}

$$\begin{aligned} J_{eq} &= J_e + G_{e2g}^2 J_g' \\ J_{gc} &= \frac{G_{e2g} G_{i2g}}{G_{f2m}} J_g' \\ J_{mq} &= J_m + \frac{G_{i2g}^2}{G_{f2m}^2} J_g'. \end{aligned} \tag{A15}$$

The GM EVT in mode-2 has additional parameter definitions. The motor, M/G2, shaft inertia given in (A13) in mode 1 now includes additional terms due to the exercising of CL3

$$\begin{aligned} J_{mot\_sh} = J_{mg2} + J_{S2} + \frac{1}{G_{f2m}^2} \left(J_{fd} + \frac{1}{G_{a2f}^2} J_a \right) \\ + \frac{1}{G_{r2m}^2} (J_{R2} + J_{S1} + J_{mg1}). \end{aligned} \tag{A16}$$

The equivalent lumped inertias of (A15) are also modified by the system structure change

$$\begin{aligned} J_{eq} &= J_e - \left(G_{e2g}^2 + \frac{G_{i2g} G_{r2m} G_{e2g}^2}{G_{f2m} + G_{r2m} G_{i2g}} \right) J_g' \\ J_{gc} &= \frac{G_{e2g} G_{i2g}}{G_{f2m} + G_{r2m} G_{i2g}} J_g' \\ J_{mq} &= \left(J_m - \frac{1}{G_{r2m} G_{e2g}} J_{gc} + \frac{G_{r2m} G_{i2g}}{G_{f2m} + G_{r2m} G_{i2g}} J_g' \right). \end{aligned} \tag{A17}$$

Last, an additional modification to J_{eq} of (A17) will arise in the derivation of driveline torque under mode 2 as

$$J_{eq2} = \frac{1}{G_{r2m} G_{e2g}} J_{eq} - G_{r2m} G_{e2g} J_g' - G_{r2m}^2 J_{gc}. \tag{A18}$$

REFERENCES

[1] J. M. Miller, "Propulsion systems for hybrid vehicles," *IEE Power & Energy Series* vol. 45, Dec. 2003 [Online]. Available: www.iee.org/books, PO045

[2] J. M. Miller, P. J. McCleer, M. Everett, and E. Strangas, "Ultracapacitor plus battery energy storage system sizing methodology for HEV power split electronic CVTs," in *Proc. IEEE Int. Symp. Ind. Electron. (ISIE'05)*, Dubrovnik, Croatia, Jun. 20–23, 2005, pp. 317–324.

[3] J. M. Miller, P. J. McCleer, and M. Everett, "Comparative assessment of ultracapacitors and advanced battery energy storage systems in power split electronic CVT vehicle power trains," in *Proc. IEEE Int. Elect. Machines Drives Conf. (IEMDC'05)*, San Antonio, TX, May 15–18, 2005, pp. 1513–1520.

[4] J. M. Miller and M. Everett, "An assessment of ultracapacitors as the power cache in Toyota THS-II, GM-Allison AHS-2 and Ford FHS hybrid propulsion systems," in *Proc. IEEE App. Power Electron. Conf. Exhibition (APEC'05)*, Austin, TX, Mar. 6–10, 2005, pp. 481–490.

[5] D. Fussner and Y. Singh, "Development of single stage input coupled split power transmission arrangements and their characteristics," presented at the SAE World Congr., Detroit, MI, Mar. 4–7, 2002.

[6] R. Wohl, T. Long, Jr., V. Mucino, and J. E. Smith, "A model for a planetary-CVT mechanism: analysis and synthesis," in *Proc. SAE Congress Expo*, Detroit, MI, Mar. 1993, pp. 1–11.

[7] V. H. Mucino, J. E. Smith, B. Cowan, and M. Kmicikiewicz, "Parametric modeling and analysis of a planetary gear-CVT mechanism," in *Proc. SAE Congress Expo*, Detroit, MI, Feb. 28–Mar. 3 1994, p. 51.

[8] H. Zhang, Y. Zhu, G. Tian, Q. Chen, and Y. Chen, "Optimal energy management strategy for hybrid electric vehicles," presented at the SAE Congress, Detroit, MI, Mar. 2004.

[9] A. G. Holmes and M. R. Schmidt, "Hybrid Electric Powertrain Including a Two-Mode Electrically Variable Transmission," U.S. Patent 6 478 705 B1, Nov. 12, 2002.

[10] X. Ai, T. Mohr, and S. Anderson, "An electro-mechanical infinitely variable speed transmission," presented at the Proc. SAE Congress Expo, 2004.

[11] A. Villeneuve, "Dual mode electric infinitely variable transmission," in *Proc. SAE TOPTECH Meeting Continuously Variable Transm.*, 2004, pp. 1–11.

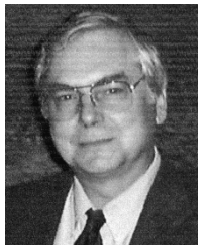

John M. Miller (M'82–SM'94–F'99) received the B.S.E.E. degree from the University of Arkansas, Fayetteville, in 1976, the M.S.E.E. degree from Southern Methodist University, Dallas, TX, in 1979, and the Ph.D. degree from Michigan State University, East Lansing, in 1983.

He is Founder and President of J-N-J Miller Design Services, P.L.C., Cedar, MI, where he is Principal Engineer. Previously, he was a Member of Technical Staff at Texas Instruments, Dallas, TX, from 1976 to 1980. He joined Ford Motor Company Research in 1983 to work on electric and hybrid vehicle programs. He has worked in the white goods industry where he applied embedded controls to appliances and in technical consulting with Exponent Failure Analysis Associates. He became an Adjunct Professor at Michigan State University, East Lansing, in 1998 and an Adjunct Professor at Texas A&M University, College Station, in 2002. He is an Outside Representative on the MIT-Industry Consortium on Advanced Automotive Electrical and Electronic Systems and Components. He is the holder of 50 US patents and has authored more than 120 publications on automotive electrical and electronic systems. He is co-author of *Handbook of Automotive Power Electronics and Motor Drives* (New York: Marcel Dekker, 2004) and *Vehicular Electric Power Systems: Land, Sea, Air, and Space Vehicles* (New York: Marcel Dekker, 2003). He is author of *Propulsion Systems for Hybrid Vehicles* (London, U.K.: IEE Press, 2003).

Dr Miller received the Best Paper Award from the IEEE Vehicular Technology Society, the Most Outstanding Paper by IEEE and SAE Convergence in 2000, the Henry Ford Technology Award for the development of the starter-alternator system for hybrid vehicles, and the IEEE Third Millenium Medal. He is currently Editor-in-Chief of the *IEEE Power Electronics Society Newsletter* and Chairman of the Education and Outreach Committee, KiloFarad International. He is an IEEE Power Electronics Society Distinguished Lecturer and a Registered Professional Engineer in in the state of Michigan.